RESONANCE LINE TRANSFER AND TRANSPORT OF EXCITED ATOMS—III. SELF-CONSISTENT SOLUTIONS (2)

O. Atanacković,[1] J. Borsenberger,[2] J. Oxenius[3]† and E. Simonneau[4]

[1]Astronomska Opservatorija, Volgina 7, 11050 Beograd, Yugoslavia, [2]Département de Recherches Spatiales, Observatoire de Paris-Meudon, F-92195 Meudon Principal Cedex, France, [3]Université Libre de Bruxelles, Campus Plaine, C.P. 231, B-1050 Bruxelles, Belgium, Association Euratom-Etat Belge, and [4]Institut d'Astrophysique, Laboratoire d'Astrophysique Théorique du Collège de France, 98 bis Bd. Arago, F-75014 Paris, France

Abstract—In this last part of our study on non-LTE line transfer with convective transport of excited atoms, we present self-consistent solutions of the radiative transfer equation and the kinetic equation of the excited two-level atoms when the excited atoms undergo elastic velocity-changing collisions. We assume pure Doppler broadening of the spectral line and investigate reflecting and destroying boundaries for the excited atoms. Concerning elastic collisions of the excited atoms, our study covers all cases, from a collisionless gas (free particle streaming) discussed in Part II of this series of papers to a collision-dominated gas with the limiting case of complete redistribution. We present arguments that the streaming pattern of the gas of excited atoms does not depend critically on the shape of the line profile. Therefore, our results for a pure Doppler profile may also be used for other line profiles (Voigt, Lorentz) in first approximation, at least when the streaming parameter η is not too large.

1. INTRODUCTION

In two previously published papers,[1,2] in the following referred to as Parts I and II,‡ we considered non-LTE line transfer by two-level atoms when streaming of excited atoms is taken into account. In particular, in Part II we presented self-consistent solutions of the transfer equation for the radiation intensity $I_\nu(\mathbf{n})$ and the kinetic equation for the distribution function of excited atoms $F_2(\mathbf{v})$ for the limiting case when the excited atoms do not undergo elastic velocity-changing collisions (free particle streaming). In this Part III, we take these elastic collisions into account. Hence, we must now deal with all three dimensionless parameters ϵ, ζ, η [Eqs. (II.2.1–3)] which characterize, respectively, inelastic collisions, elastic collisions, and streaming of the excited atoms. By constrast, only two parameters ϵ and η were used in Part II.

Quite generally, elastic velocity-changing collisions of excited atoms affect the radiation transport in a spectral line in two distinct ways.[3,4] Firstly, strong collisions that lead to large momentum transfer between the collision partners give rise to complete redistribution in the atomic rest frame, which means that the atomic emission profile $\eta_{21}(\xi)$ equals the atomic absorption profile $\alpha_{12}(\xi)$. Secondly, elastic collisions affect the velocity distribution of excited atoms $f_2(\mathbf{v})$. As can be seen from Eq. (I.2.17), both effects influence the line emission profile ψ_ν, and hence the radiative transfer in the spectral line considered. For the case of pure Doppler broadening considered in this paper, the equality $\eta_{21}(\xi) = \alpha_{12}(\xi)$ is always valid [Eq. (I.2.1)], so that here elastic collisions affect the line emission profile only via the velocity distribution $f_2(\mathbf{v})$. In our model, the excited atoms undergo elastic collisions with nonexcited atoms having a velocity distribution that is Maxwellian of temperature T (see Sec. I.2.1). These elastic collisions therefore tend to make $f_2(\mathbf{v})$ Maxwellian of temperature T. In particular, the macroscopic mean velocity of the excited atoms is normally less than for the collisionless case. However, near a boundary that destroys the excited atoms, the flow velocity into the boundary is always of the same order as the thermal velocity of the atoms (see Secs. 4.3 and 5.2; cf. also Sec. I.5.6).

The present paper is organized as follows. After recalling in Sec. 2 the governing equations, we present in Sec. 3 numerical solutions for the static case where streaming of excited atoms is

†To whom all correspondence should be addressed.
‡Equations and sections of these papers are referred to as Eq. (I.2.50) and Sec. II.6.1.

neglected ($\eta = 0$, $\zeta \neq 0$). In Sec. 4, we investigate the general case of non-LTE line transfer with convective transport of excited atoms in the presence of elastic collisions ($\eta \neq 0$, $\zeta \neq 0$). Finally, in Sec. 5, we introduce the diffusion approximation for elastic collision-dominated gases characterized by the inequalities $\zeta \gg 1$ and $\eta/\zeta \ll 1$.

2. GOVERNING EQUATIONS

For easy reference we collect in this section the governing equations of our model. The main physical assumptions underlying our study have been summarized at the beginning of Sec. II.2.

The radiative transfer equation for the specific intensity $I_x(\mathbf{n}) \equiv I_x(\mu)$, where $\mu \equiv \mathbf{n} \cdot \mathbf{e}_z$, remains unchanged [cf. Eq. (II.2.7)],

$$\mu(d/d\tau)I_x(\mu;\tau) = \varphi_x I_x(\mu;\tau) - n_2(\tau)\psi_x(\mu;\tau). \tag{2.1}$$

Here, φ_x denotes the Gaussian line absorption coefficient [cf. Eq. (II.2.8)]

$$\varphi_x = \pi^{-1/2}\exp(-x^2), \tag{2.2}$$

and the line emission coefficient $n_2\psi_x$ is given by [cf. Eq. (II.2.9)]

$$n_2(\tau)\psi_x(\mu;\tau) = \int F_2(\mathbf{y};\tau)\delta(x - \mathbf{n}\cdot\mathbf{y})\,d^3y. \tag{2.3}$$

The normalized emission profile $\psi_x(\mathbf{n}) \equiv \psi_x(\mu)$ obeys the symmetry relation [cf. Eqs. (I.6.5) and (II.3.35)]

$$\psi_x(\mathbf{n};\tau) = \psi_{-x}(-\mathbf{n};\tau), \quad \psi_x(\mu;\tau) = \psi_{-x}(-\mu;\tau). \tag{2.4}$$

On the other hand, if the excited two-level atoms undergo elastic velocity-changing collisions with nonexcited two-level atoms, the kinetic equation for the distribution function $F_2(\mathbf{y}) \equiv F_2(y,\mu)$, where $\mu \equiv \mathbf{y} \cdot \mathbf{e}_z/y$, now takes the form [cf. Eq. (I.2.50)]

$$\eta y\mu(d/d\tau)F_2(y,\mu;\tau) = F_2(y,\mu;\tau) - [\epsilon + (1-\epsilon)I_{12}(y,\mu;\tau)]f^M(y) - \zeta[n_2(\tau)f^M(y) - F_2(y,\mu;\tau)] \tag{2.5a}$$

or

$$\eta y\mu(1+\zeta)^{-1}(d/d\tau)F_2(y,\mu;\tau) = F_2(y,\mu;\tau) - (1+\zeta)^{-1}[\epsilon + (1-\epsilon)I_{12}(y,\mu;\tau) + \zeta n_2(\tau)]f^M(y), \tag{2.5b}$$

which for $\zeta = 0$ reduce to Eq. (II.2.10). Here,

$$f^M(y) = \pi^{-3/2}\exp(-y^2) \equiv \pi^{-3/2}\exp(-\mathbf{y}\cdot\mathbf{y}) \tag{2.6}$$

is the normalized three-dimensional Maxwell distribution [cf. Eq. (II.2.12)], while $I_{12}(\mathbf{y}) \equiv I_{12}(y,\mu)$ is defined by [cf. Eq. (II.2.11)]

$$I_{12}(y,\mu;\tau) = \iint I_x(\mathbf{n};\tau)\delta(x - \mathbf{n}\cdot\mathbf{y})\,dx\,d\Omega/4\pi. \tag{2.7}$$

From $I_{12}(\mathbf{y})$ is derived the quantity [cf. Eqs. (II.3.23) and (II.3.42)]

$$J_{12}(\tau) = \int I_{12}(\mathbf{y};\tau)f^M(y)\,d^3y = \iint I_x(\mathbf{n};\tau)\varphi_x\,dx\,d\Omega/4\pi. \tag{2.8}$$

Equation (2.5b) is the balance equation for the excited atoms of velocity $\mathbf{y}$ at the optical depth τ. The left-hand side describes the streaming of these atoms, and the right-hand side their net production. More specifically, the first term of the r.h.s. describes the destruction of excited atoms of velocity $\mathbf{y}$ through de-excitation collisions, spontaneous emissions, and elastic collisions, while the second term of the r.h.s. describes the creation of such atoms through excitation collisions (ϵ), absorptions (I_{12}), and elastic collisions (ζn_2). Due to our definition of the optical depth variable τ [see Eq. (I.2.48)], the destruction term here has a plus sign, and the creation term a minus sign.

The boundary conditions are unchanged. Since $\tau = \frac{1}{2}\tau^0$ is a symmetry plane, one has [cf. Eq. (II.2.13)]

$$(d/d\tau)I_x(\mu; \tau = \tfrac{1}{2}\tau^0) = (d/d\tau)F_2(y, \mu; \tau = \tfrac{1}{2}\tau^0) = 0. \tag{2.9}$$

At $\tau = 0$, the photons escape from the system, so that [cf. Eq. (II.2.14)]

$$I_x^-(\mu; \tau = 0) = 0, \tag{2.10}$$

while, for the excited atoms, a reflecting boundary corresponds to [cf. Eq. (II.2.15)]

$$F_2^-(y, \mu; \tau = 0) = F_2^+(y, \mu; \tau = 0), \tag{2.11}$$

and a destroying boundary to [cf. Eq. (II.2.16)]

$$F_2^-(y, \mu; \tau = 0) = 0. \tag{2.12}$$

3. THE STATIC CASE

We first consider the static case where no streaming of excited atoms occurs ($\eta = 0$). Here, the limiting case of no elastic collisions $\zeta = 0$ corresponds to static partial redistribution as discussed in Sec. II.4. The opposite limiting case $\zeta = \infty$ leads to a Maxwellian velocity distribution $f_2(y) = f^M(y)$ and thus to complete redistribution, $\psi_x = \varphi_x$. Not surprisingly, the general case of a finite $\zeta \neq 0$ may formally be viewed as a superposition of static partial redistribution and complete redistribution, as will now be shown.

For $\eta = 0$, Eq. (2.5b) gives the distribution function F_2 in terms of the radiation intensity I_x as

$$F_2(y) = (1 + \zeta)^{-1}[\epsilon + (1 - \epsilon)I_{12}(y) + \zeta n_2]f^M(y), \tag{3.1}$$

which upon integration $\int d^3y$ yields

$$n_2 = \epsilon + (1 - \epsilon)J_{12} \tag{3.2}$$

in view of Eqs. (2.8) and (II.3.36). Hence, Eq. (3.1) can also be written as

$$F_2(y) = n_2 f^M(y) + \frac{1 - \epsilon}{1 + \zeta}[I_{12}(y) - J_{12}]f^M(y). \tag{3.3}$$

For $\zeta = \infty$, Eqs. (3.1) and (3.3) reduce to a Maxwell distribution corresponding to complete redistribution,

$$F_2^{CR}(y) = n_2 f^M(y); \tag{3.4}$$

for $\zeta = 0$, we recover the distribution function corresponding to static partial redistribution [cf. Eqs. (II.4.1) and (II.4.4)]

$$F_2^{PR}(y) = [\epsilon + (1 - \epsilon)I_{12}(y)]f^M(y) = n_2 f^M(y) + (1 - \epsilon)[I_{12}(y) - J_{12}]f^M(y). \tag{3.5}$$

Thus, in terms of the normalized velocity distribution $f_2(y) = F_2(y)/n_2$ [Eq. (I.2.2)] or of the reduced velocity distribution $\tilde{f}_2(y) = f_2(y)/f^M(y)$ [Eq. (I.2.23)], Eq. (3.3) takes the form

$$f_2(y) = \frac{f_2^{PR}(y) + \zeta f^M(y)}{1 + \zeta}, \tilde{f}_2(y) = \frac{\tilde{f}_2^{PR}(y) + \zeta}{1 + \zeta}, \tag{3.6}$$

the interpretation of which is straightforward.

We now turn to the emission profile ψ_x. Inserting Eq. (3.3) into Eq. (2.3) and using Eq. (II.4.6) leads to the static line-emission coefficient

$$n_2\psi_x(\mathbf{n}) = n_2\varphi_x + \frac{1 - \epsilon}{1 + \zeta}\left[\int I_{12}(y)f^M(y)\delta(x - \mathbf{n}\cdot y)\,d^3y - J_{12}\varphi_x\right], \tag{3.7}$$

which can be written as

$$n_2\psi_x(\mathbf{n}) = n_2\varphi_x + \frac{1 - \epsilon}{1 + \zeta}[R_x(\mathbf{n}) - J_{12}\varphi_x] \tag{3.8}$$

in terms of the redistribution integral

$$R_x(\mathbf{n}) = \iint I_{x'}(\mathbf{n}')R_{IA}(x',\mathbf{n}';x,\mathbf{n})\,\mathrm{d}x'\,\mathrm{d}\Omega'/4\pi. \tag{3.9}$$

Here, the redistribution function R_{IA} (in Hummer's[5] notation) corresponds to isotropic, pure Doppler broadening,

$$R_{IA}(x',\mathbf{n}';x,\mathbf{n}) = \int \delta(x' - \mathbf{n}'\cdot\mathbf{y})\delta(x - \mathbf{n}\cdot\mathbf{y})f^M(y)\,\mathrm{d}^3y, \tag{3.10}$$

and obeys the relations

$$R_{IA}(x',\mathbf{n}';x,\mathbf{n}) = R_{IA}(x,\mathbf{n};x'\,\mathbf{n}'), \tag{3.11}$$

$$\iint R_{IA}(x',\mathbf{n}';x,\mathbf{n})\,\mathrm{d}x'\,\mathrm{d}\Omega'/4\pi = \varphi_x, \tag{3.12}$$

$$\iiiint R_{IA}(x',\mathbf{n}';x,\mathbf{n})\,\mathrm{d}x'\,\mathrm{d}\Omega'\,\mathrm{d}x\,\mathrm{d}\Omega/(4\pi)^2 = 1. \tag{3.13}$$

We recall that redistribution functions can be employed only in the static case in the absence of elastic collisions ($\eta = \zeta = 0$)[4].

For $\zeta = \infty$, Eq. (3.8) yields the emission coefficient of complete redistribution

$$n_2\psi_x^{CR} = n_2\varphi_x. \tag{3.14}$$

For $\zeta = 0$, Eq. (3.8) reduces to the emission coefficient corresponding to static partial redistribution

$$n_2\psi_x^{PR}(\mathbf{n}) = \epsilon\varphi_x + (1 - \epsilon)R_x(\mathbf{n}), \tag{3.15}$$

where $\epsilon\varphi_x$ and $(1 - \epsilon)R_x$ are the emission coefficients due to atoms that have been excited by excitation collisions and absorptions, respectively. Thus, in terms of the normalized emission profile $\psi_x(\mathbf{n})$ or of the reduced emission profile $\widetilde{\psi}_x(\mathbf{n}) = \psi_x(\mathbf{n})/\varphi_x$ [Eq. (I.2.29)], Eq. (3.8) takes the form

$$\psi_x(\mathbf{n}) = \frac{\psi_x^{PR}(\mathbf{n}) + \zeta\varphi_x}{1 + \zeta}, \quad \widetilde{\psi}_x(\mathbf{n}) = \frac{\widetilde{\psi}_x^{PR}(\mathbf{n}) + \zeta}{1 + \zeta}, \tag{3.16}$$

in analogy to Eq. (3.6).

It should be observed that the various derived relations are formal in the sense that the quantities $n_2(\tau)$, $f_2^{PR}(\mathbf{y};\tau)$, $\psi_x^{PR}(\mathbf{n};\tau)$ depend on the radiation intensity $I_x(\mathbf{n};\tau)$ and, therefore, depend implicitly on ζ, because the self-consistent intensity $I_x(\mathbf{n};\tau)$ depends on the parameter ζ that characterizes the gas under consideration. Hence, we should write $n_2(\tau\,|\,\zeta)$, $f_2^{PR}(\mathbf{y};\tau\,|\,\zeta)$, $\psi_x^{PR}(\mathbf{n};\tau\,|\,\zeta)$. Nevertheless, Eqs. (3.6) and (3.16) are instructive and, moreover, display the dominant dependence of f_2 and ψ_x on the parameter ζ, as opposed to the indirect, much weaker dependence on ζ through f_2^{PR} and ψ_x^{PR}.

Thus, the velocity distribution f_2 and the emission profile ψ_x corresponding to a given ζ are readily estimated using Eqs. (3.6) and (3.16) together with Figs. II.2. On the other hand, the dependence of the number density n_2 on ζ can be characterized by the quantity

$$b_\zeta(\tau) = [n_2^{CR}(\tau) - n_2(\tau\,|\,\zeta)]/n_2^{CR}(\tau), \tag{3.17}$$

where $n_2^{CR}(\tau) \equiv n_2(\tau\,|\,\zeta = \infty)$ is the density of excited atoms corresponding to complete redistribution (see Fig. II.4). It turns out that for optical depths smaller than the thermalization length, $\tau < \epsilon^{-1}$, $b_\zeta(\tau)$ is rather independent of τ, while for $\tau > \epsilon^{-1}$, $b_\zeta(\tau) \simeq 0$ of course. Table 1 lists $b_\zeta(0)$ at the surface $\tau = 0$ for various values of ϵ and ζ. As expected, the deviations of n_2 from n_2^{CR} increase with decreasing parameters ϵ and ζ.

4. THE GENERAL CASE

We now turn to the general case where both streaming of excited atoms and elastic collisions of excited atoms are taken into account ($\eta \neq 0$, $\zeta \neq 0$). Since we are interested only in non-LTE

Table 1. The quantity $b_\zeta(0)$, Eq. (3.17), at the surface $\tau = 0$ of a semi-infinite ($\tau^0 = \infty$), static ($\eta = 0$) gas layer, for various values of ϵ and ζ. The case $\zeta = 0$ corresponds to static partial redistribution (Sec. II.4.)

ϵ \ ζ	0	0.01	0.1	1	10	100
10^{-2}	0.046	0.045	0.038	0.013	0.000	0.000
10^{-4}	0.165	0.163	0.148	0.076	0.013	0.003
10^{-6}	0.245	0.242	0.221	0.118	0.021	0.003

gases, $\epsilon \ll 1$ is always understood in the following whenever a nonspecified ϵ is mentioned. As in Part II, we present numerical results for a gas layer specified by

$$\epsilon = 10^{-4}, \quad \tau^0 = 2 \times 10^6,$$

which behaves like a semi-infinite layer because its optical thickness is much larger than the thermalization length corresponding to pure Doppler broadening, $\tau^0 \gg \epsilon^{-1}$. The numerical integration of the two coupled kinetic equations (2.1) and (2.5) was performed by using the method of variable Eddington factors (see Sec. II.3). It will prove convenient to present the numerical results for the macroscopic quantities $n_2(\tau)$, $u(\tau)$, $\phi(\tau)$ of the gas of excited atoms together with the corresponding quantities that follow from the two-fluid model introduced in Sec. II.6.1 and suitably modified below to allow for the occurrence of elastic velocity-changing collisions ($\zeta \neq 0$).

4.1. Two-fluid model

The two-fluid model for a semi-infinite gas layer, introduced in Sec. II.6.1, replaces the distribution function $F_2(\mathbf{y}; \tau)$ and the radiation intensity $I_x(\mathbf{n}; \tau)$ by two functions $F^+(\tau)$, $F^-(\tau)$ and $I^+(\tau)$, $I^-(\tau)$, respectively, that describe the "outgoing" and "incoming" atoms and photons in a first approximation. In this model, elastic collisions are taken into account by replacing Eqs. (II. 6.1a,b) by

$$\eta \bar{y} \bar{\mu}' \, dF^+/d\tau = (1 + \zeta)F^+ - [\epsilon + (1 - \epsilon)J_{12} + \zeta n_2], \tag{4.1a}$$

$$-\eta \bar{y} \bar{\mu}' \, dF^-/d\tau = (1 + \zeta)F^- - [\epsilon + (1 - \epsilon)J_{12} + \zeta n_2], \tag{4.1b}$$

in view of Eq. (2.5a). On the other hand, the transfer equation (II.6.2), the definition of the various moments, Eqs. (II.6.4,5), and the boundary conditions (II.6.6–8) remain unchanged. We recall that $\mu' = \mathbf{y} \cdot \mathbf{e}_z / y$ and $\mu = \mathbf{n} \cdot \mathbf{e}_z$ here denote the direction cosines with respect to the z-axis of the atomic velocity $\mathbf{y}$ and the photon direction $\mathbf{n}$, respectively.

Defining

$$\alpha_c = \alpha(1 + \zeta)^{-1/2} = \eta \bar{y} \bar{\mu}'(1 + \zeta)^{-1/2}, \quad \beta = \bar{\mu}/\varphi_{\bar{x}}, \tag{4.2}$$

we readily derive for the moments n_2 and J_{12} the relations [cf. Eqs. (II.6.10–15)]

$$\alpha_c^2 n_2''(\tau) = n_2(\tau) - [\epsilon + (1 - \epsilon)J_{12}(\tau)], \tag{4.3}$$

$$\beta^2 J_{12}''(\tau) = J_{12}(\tau) - n_2(\tau), \tag{4.4}$$

$$n_2(\infty) = J_{12}(\infty) = 1, \tag{4.5}$$

$$\alpha_c n_2'(0) = \gamma n_2(0); \quad \gamma^R = 0; \quad \gamma^D = (1 + \zeta)^{1/2}, \tag{4.6}$$

$$\beta J_{12}'(0) = J_{12}(0), \tag{4.7}$$

$$\phi(\tau) = (\alpha_c^2/\eta)n_2'(\tau); \quad u(\tau) = \phi(\tau)/n_2(\tau). \tag{4.8}$$

In Eq. (4.6), the superscripts R and D refer to reflecting and destroying boundaries, respectively. Comparison with Eqs. (II.6.10–15) shows that the only changes concern the replacement $\alpha \rightarrow \alpha_c$ and the appearance of the factor $\gamma^D = (1 + \zeta)^{1/2}$ rather than $\gamma^D = 1$ for a destroying boundary.

Concerning the representative values $\bar{y}$, $\bar{\mu}'$ for the excited atoms and $\bar{x}$, $\bar{\mu}$ for the photons, we adopt the same values as in Sec. II.6.1. As discussed there, this choice leads to too small values

of the thermalization length L_T and, for $\eta > 1$, of the streaming length L_S, but, leaving aside the absolute magnitudes of L_T and L_S, it describes adequately the streaming of excited atoms which primarily arises in the surface layer $0 < \tau < L_S$. Thus, in our model [cf. Eq. (II.6.21)],

$$\alpha_c = 2^{-1/2}\eta(1 + \zeta)^{-1/2}, \quad \beta = 1/3^{1/2}\varphi_{\tilde{x}} \sim 1. \tag{4.9}$$

By analogy to Eq. (II.6.27), we also introduce the quantity

$$\omega_c = \alpha_c/\beta = \omega(1 + \zeta)^{-1/2} = \eta/2^{1/2}\beta(1 + \zeta)^{1/2}. \tag{4.10}$$

Therefore, in our two-fluid model, the following orders of magnitude arise:

$$\alpha_c \sim \omega_c \sim \eta(1 + \zeta)^{-1/2}, \quad \beta \sim 1. \tag{4.11}$$

However, as in Part II, we keep in our formulas the parameter β in order to display explicitly the influence of the representative photon frequency $\tilde{x}$ on the results obtained.

The thermalization length L_T and the streaming length L_S are the positive roots of the characteristic equation corresponding to Eqs. (4.3) and (4.4,), that is, of Eq. (II.6.24) with α replaced by α_c. Thus, for $\epsilon \ll 1$ and in the presence of elastic collisions $\zeta \neq 0$, one obtains in analogy to Eqs. (II.6.25) and (II.6.26)

$$L_T = \epsilon^{-1/2}(\alpha_c^2 + \beta^2)^{1/2} = \epsilon^{-1/2}\beta(1 + \omega_c^2)^{1/2}, \tag{4.12}$$

$$L_S = \alpha_c\beta(\alpha_c^2 + \beta^2)^{-1/2} = \alpha_c(1 + \omega_c^2)^{-1/2} = \beta\omega_c(1 + \omega_c^2)^{-1/2}. \tag{4.13}$$

Comparison with the following numerical results will show that (as for the collisionless case $\zeta = 0$) using the orders of magnitude (4.11) in Eqs. (4.12) and (4.13) leads to too small a thermalization length L_T, and that the correct streaming length L_S is obtained only if $\omega_c < 1$. The scale lengths L_T and L_S will further be discussed in Sec. 6.

However, the great merit of Eqs. (4.12) and (4.13) consists in displaying the functional dependence of L_T and L_S on the parameters ϵ, η, ζ. First, from the relation

$$L_S/L_T = \epsilon^{1/2}\omega_c/(1 + \omega_c^2) < \epsilon^{1/2},$$

we conclude that $L_S \ll L_T$ in non-LTE gases with $\epsilon \ll 1$; as stated repeatedly, in our model $L_T \sim \epsilon^{-1/2}$ rather than $L_T \sim \epsilon^{-1}$.

Next, Eqs. (4.12) and (4.13) predict both L_T and L_S to decrease with increasing elastic collision frequency, that is, with increasing ζ. This result is most easily seen by writing

$$L_T = \epsilon^{-1/2}\beta[1 + \omega^2/(1 + \zeta)]^{1/2}, \quad L_S = \alpha(1 + \zeta + \omega^2)^{-1/2},$$

where α and ω [cf. Eqs. (II.6.21) and (II.6.27)] correspond to the collisionless case $\zeta = 0$, and are hence independent of ζ.

In the limiting case $\omega_c \ll 1$ where streaming is not very important, one obtains from Eqs. (4.12) and (4.13)

$$L_T \sim \epsilon^{-1/2}\beta, \quad L_S \sim \alpha_c \sim \eta(1 + \zeta)^{-1/2}. \tag{4.14}$$

Thus, L_T here is independent of η and ζ, as expected, while L_S depends on these parameters through the characteristic combination $\alpha_c \sim \omega_c \sim \eta(1 + \zeta)^{-1/2}$.

In the opposite limiting case $\omega_c \gg 1$ where streaming is important, Eqs. (4.12) and (4.13) yield

$$L_T \sim \epsilon^{-1/2}\beta\omega_c \sim \epsilon^{-1/2}\eta(1 + \zeta)^{-1/2}, \quad L_S \sim \beta. \tag{4.15}$$

Here, the thermalization length increases with increasing parameter ω_c. In terms of the parameters η and ζ, L_T increases with increasing η, and decreases with increasing ζ, as expected on physical grounds. On the other hand, for $\omega_c \gg 1$, the two-fluid model with the choice of parameters (4.11) leads to a streaming length $L_S \sim \beta \sim 1$ independently of η and ζ (see also Sec. II.6.1).

In the two-fluid model with elastic collisions, the particle and photon moments that are solutions of Eqs. (4.3)–(4.8) can be written as [cf. Eqs. (II.6.28–30)]

$$n_2(\tau) = 1 - A_T\exp(-\tau/L_T) - A_S\exp(-\tau/L_S), \tag{4.16}$$

$$\phi(\tau) = 2^{-1/2}[l_T A_T\exp(-\tau/L_T) + l_S A_S\exp(-\tau/L_S)], \tag{4.17}$$

$$J_{12}(\tau) = 1 - [A_T/(1 - k_T^2)]\exp(-\tau/L_T) - [A_S/(1 - k_S^2)]\exp(-\tau/L_S). \tag{4.18}$$

Here, the characteristic lengths L_T and L_S are defined by Eqs. (4.12) and (4.13). The coefficients A_T^R, A_S^R, A_T^D, A_S^D are again given by Eqs. (II.6.35)–(II.6.38). However, k_T, l_T, k_S, l_S are now given by

$$k_T = \beta/L_T = \epsilon^{1/2}/(1 + \omega_c^2)^{1/2},$$ (4.19)

$$l_T = \alpha_c/L_T(1 + \zeta)^{1/2} = \epsilon^{1/2}\omega_c/(1 + \omega_c^2)^{1/2}(1 + \zeta)^{1/2},$$ (4.20)

$$k_S = \beta/L_S = (1 + \omega_c^2)^{1/2}/\omega_c,$$ (4.21)

$$l_S = \alpha_c/L_S(1 + \zeta)^{1/2} = (1 + \omega_c^2)^{1/2}/(1 + \zeta)^{1/2}.$$ (4.22)

For $\zeta = 0$, they reduce to Eqs. (II.6.31–34). Again, $k_T, l_T < \epsilon^{1/2}$ and $k_S > 1$, but now $l_S \gtrless 1$ as opposed to $l_S > 1$ in the collisionless case $\zeta = 0$.

4.2. Reflecting boundary

We first consider a gas enclosed between boundaries that reflect the excited atoms. In this case, the effect of elastic velocity-changing collisions of excited atoms can be summarized by saying that they tend to thermalize the velocity distribution $f_2(\mathbf{v})$ at each point of the gas (in contrast to the case of destroying boundaries, see Sec. 4.3). In other words, with increasing parameter ζ, one approaches static complete redistribution where, in particular, $u(\tau)$ and $\phi(\tau)$ vanish identically.

For reflecting boundaries, the formulas corresponding to the two-fluid model in the presence of elastic collisions are obtained from those of the collisionless case by replacing ω by ω_c, and by multiplying the formulas for $\phi(\tau)$ and $u(\tau)$ by the factor $(1 + \zeta)^{-1/2}$. Thus, formally, in the expressions of Sec. II.6.2, we must make the substitutions

$$\omega \to \omega_c, \quad \phi^R(\tau) \to (1 + \zeta)^{1/2}\phi^R(\tau), \quad u^R(\tau) \to (1 + \zeta)^{1/2}u^R(\tau),$$

ω_c being defined in Eq. (4.10).

Let us first consider the case $\eta \lesssim 1$. Here, the transport of excited atoms from deeper layers into the boundary region more or less compensates the decrease of the density n_2 there that is due to partial redistribution (see Fig. II.4), resulting in a density distribution $n_2(\tau)$ which resembles that of complete redistribution (see Fig. II.5). As a result, elastic collisions hardly affect $n_2(\tau)$ if $\eta \lesssim 1$, because even the limiting distributions $n_2(\tau)$ corresponding to $\zeta = 0$ (partial redistribution) and $\zeta = \infty$ (complete redistribution) practically do not differ from each other. On the other hand, the mean velocity $u(\tau)$ decreases with increasing parameter ζ according to the scaling law $(1 + \zeta)^{-1/2}$. For these reasons, we do not illustrate this case by figures.

To illustrate the effect of elastic collisions in the more interesting situation $\eta \gg 1$, we choose the case $\eta = 100$. In the collisionless case $\zeta = 0$, the increase of the thermalization length due to streaming and partial redistribution is clearly visible on the $n_2(\tau)$ distribution (see Fig. II.5). On the other hand, for $\eta = 100$ and $\zeta = 0$, the mean velocity $u(\tau)$ as a function of optical depth has two maxima (see Fig. II.7), the origin or which was discussed in Sec. II.5. The evolution of these two characteristic features with increasing ζ can be followed in Figs. 1 and 2.
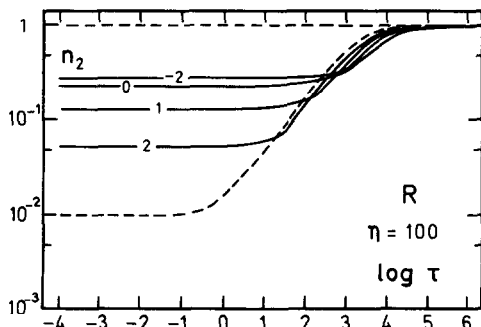

Fig. 1. Density of excited atoms n_2 vs optical depth τ of a gas layer for $\epsilon = 10^{-4}$, $\eta = 100$, $\tau^0 = 2 \times 10^6$, with reflecting boundaries. Curve labeled n $(n = -2, \ldots, 2)$ corresponds to $\zeta = 10^n$; dashed curve to $\zeta = \infty$ (complete redistribution).
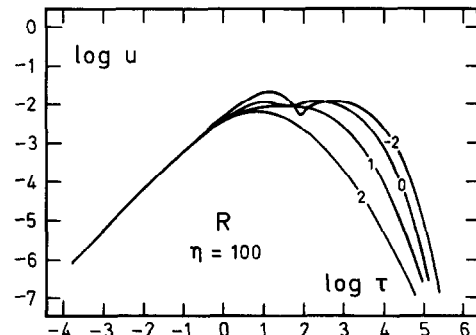
Fig. 2. Mean velocity of excited atoms u vs optical depth τ of a gas layer with $\epsilon = 10^{-4}$, $\eta = 100$, $\tau^0 = 2 \times 10^6$, with reflecting boundaries. Curve labeled n $(n = -2, \ldots, 2)$ corresponds to $\zeta = 10^n$.

The density distributions plotted in Fig. 1 show a one-exponential decay [cf. Eq. (II.6.44)] with a thermalization length that decreases with increasing ζ, approaching for $\zeta \to \infty$ the value ϵ^{-1} corresponding to complete redistribution. According to the two-fluid model, the surface density is given by [cf. Eq. (II.6.39)]

$$n_2^R(0) = \frac{\epsilon^{1/2}}{(1 + \omega_c^2)^{1/2} - \omega_c + \epsilon^{1/2}\omega_c/(1 + \omega_c^2)^{1/2}},$$ (4.23)

in reasonable agreement with the numerical results (see Fig. 1). In particular, for given ζ, $\eta \to \infty$ corresponds to $\omega_c \to \infty$, and Eq. (4.23) leads to $n_2^R(0) = 1$ corresponding to LTE, while for given η, $\zeta \to \infty$ corresponds to $\omega_c \to 0$, and Eq. (4.23) leads to $n_2^R(0) = \epsilon^{1/2}$ corresponding to complete redistribution.

In Fig. 2, the mean velocity $u(\tau)$ is plotted for the same values of η and ζ as in Fig. 1. The two maxima of $u(\tau)$ occurring for $\zeta \ll 1$ disappear with increasing ζ as a consequence of the thermalization of the velocity distribution $f_2(\mathbf{v})$ by elastic collisions. According to the two-fluid model, the mean velocity in the boundary region $0 < \tau < L_S$ is given by [cf. Eq. (II.6.49)]

$$u^R(\tau) = \frac{1}{2^{1/2}\beta(1 + \zeta)^{1/2}}[(1 + \omega_c^2)^{1/2} - \omega_c]\tau.$$ (4.24)

In the limiting case $\omega_c \gg 1$, which applies to all cases shown in Fig. 2, this reduces to

$$u^R(\tau) \simeq (1/2\eta)\tau$$ (4.25)

.ndependently of ζ. Equation (4.25), which coincides with Eq. (II.6.51), is in good agreement with the numerical results (see Fig. 2). The corresponding maximum velocity, occurring at $\tau \simeq L_S$, is given by [cf. Eq. (II.6.52)]

$$u_M^R \simeq \frac{2^{-1/2}}{(1 + \zeta)^{1/2}}\frac{\omega_c}{(1 + \omega_c^2)^{1/2}}[(1 + \omega_c^2)^{1/2} - \omega_c],$$ (4.26)

reducing for $\omega_c \gg 1$ to

$$u_M^R \simeq \beta/2\eta \simeq 1/2\eta$$ (4.27)

independently of ζ, which is in reasonable agreement with the numerical results (see Fig. 2).

Turning now to the reduced velocity distribution $\tilde{f}_2(\mathbf{v}) \equiv f_2(\mathbf{y})/f^M(y)$ and the reduced emission profile $\tilde{\psi}_x(\mu) \equiv \psi_x(\mu)/\varphi_x$, we discuss only the latter quantity since the general features of $\tilde{f}_2$ are quite analogous to those of $\tilde{\psi}_x$. In analogy to Fig. II. 10, Fig. 3 plots $\tilde{\psi}_x(\mu)$ at the optical depth $\tau = 1$
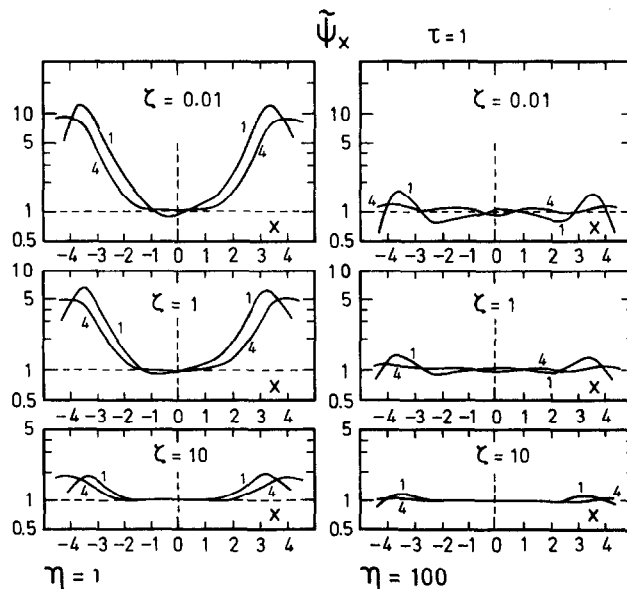

Fig. 3. Reduced emission profile $\tilde{\psi}_x(\mu)$ vs frequency x of a gas layer $\epsilon = 10^{-4}$, $\tau^0 = 2 \times 10^6$, with reflecting boundaries at the optical depth $\tau = 1$, for $\eta = 1$ and 100, and for various values of ζ. Curves labeled 1(4) correspond to $\mu_1 = 0.875$ ($\mu_4 = 0.125$). For negative μ's, use $\tilde{\psi}_x(\mu) = \tilde{\psi}_{-x}(-\mu)$, Eq. (2.4).
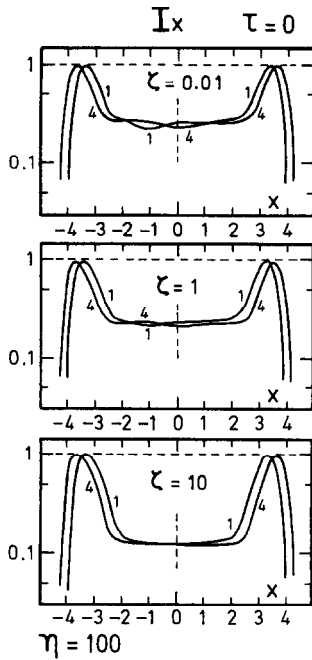
Fig. 4. Emerging intensity $I_x(\mu; \tau = 0)$ vs frequency x of a gas layer $\epsilon = 10^{-4}$, $\eta = 100$, $\tau^0 = 2 \times 10^6$, with reflecting boundaries, for various values of ζ. Curves labeled 1(4) correspond to $\mu_1 = 0.875$ $(\mu_4 = 0.125)$.
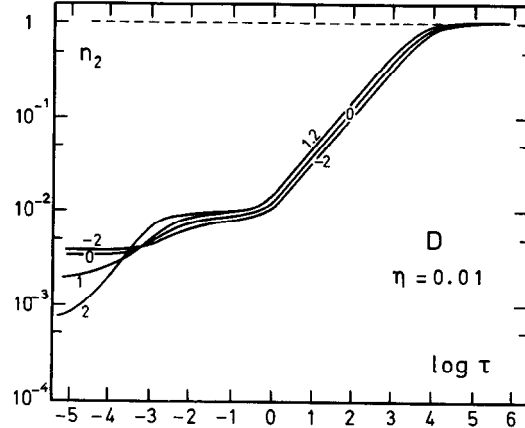
Fig. 5 Density of excited atoms n_2 vs optical depth τ of a gas layer $\epsilon = 10^{-4}$, $\eta = 0.01$, $\tau^0 = 2 \times 10^6$, with destroying boundaries. Curve labeled n ($n = -2, \ldots, 2$) corresponds to $\zeta = 10^n$.

for $\eta = 1$ and 100, respectively. We recall that $\tilde{\psi}_x$ is largely independent of η as long as $0 < \eta \lesssim 1$. On the other hand, for given ζ, $\tilde{\psi}_x(\mu; \tau)$ varies very little in the interval $0 < \tau \lesssim 1$, while it thermalizes rapidly for $\tau > 1$. Figure 3 shows that elastic collisions lead to an approach to complete redistribution, as expected. As in the collisionless case (see Fig. II. 10), the emission profile $\tilde{\psi}_x$ for $\eta = 100$ is always flatter than that for $\eta = 1$ as a consequence of the much flatter $n_2(\tau)$ distribution for $\eta = 100$ (see Fig. II.5).

The emergent intensity for small values of η, $0 < \eta \lesssim 1$, is hardly affected by elastic collisions, and practically coincides with the emergent intensities corresponding to static complete and partial redistribution which do not differ very much from each other. On the other hand, Fig. 4 shows the emergent intensity for the case $\eta = 100$. Here, elastic collisions strongly affect the emitted spectral line via their influence on the density distribution $n_2(\tau)$ (see Fig. 1). For $\zeta > 10$, the emergent intensities strongly resemble that for $\zeta = 10$ except that the intensity in the line core is determined by the corresponding surface value $n_2(0)$ (see Fig. 1).

4.3. Destroying boundary

The streaming pattern of a gas of excited atoms enclosed between destroying boundaries differs significantly from that of a gas between reflecting boundaries. Indeed, the excited atoms stream into a destroying boundary with a macroscopic velocity that is of the order of the thermal speed of the atoms (cf. Figs. I.2 and II.7), whereas the macroscopic velocity at a reflecting boundary vanishes. In this section we investigate the streaming pattern of the gas of excited atoms in the presence of destroying boundaries as a function of the collision parameter ζ, for the streaming parameters $\eta = 0.01$ and 100, respectively.

In Fig. 5 we plot the density $n_2(\tau)$ for the case $\eta = 0.01$. For $\eta \ll 1$, the surface layer in which streaming due to particle destruction at the boundary occurs is clearly visible. With increasing collision frequency, both the thickness L_S of this surface layer and the surface density $n_2(0)$ decrease. The decrease of L_S with increasing ζ is approximately described by the two-fluid model, Eq. (4.14), while the corresponding decrease of $n_2(0)$ is a consequence of the fact that elastic collisions make the velocity distribution f_2 more isotropic so that fewer atoms arrive at the boundary when ζ is increased (cf. Sec. I.5.6). As seen in Fig. 5, also the thermalization length L_T
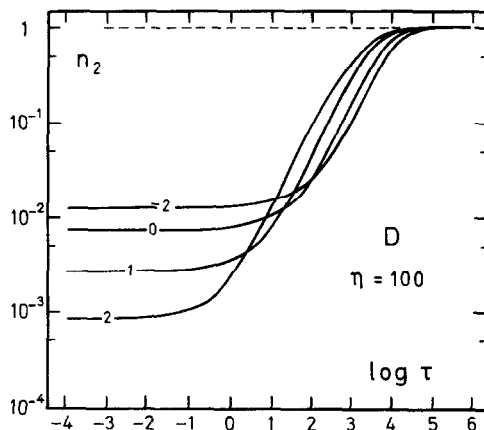
Fig. 6. Density of excited atoms n_2 vs optical depth τ of a gas layer with $\epsilon = 10^{-4}$, $\eta = 100$, $\tau^0 = 2 \times 10^6$, and destroying boundaries. Curve labeled n ($n = -2, \ldots, 2$) corresponds to $\zeta = 10^n$.

decreases slightly with increasing ζ due to the destruction of partial redistribution by elastic collisions, and therefore not accounted for by the two-fluid model [cf. Eq. (4.14)].

On the other hand, for $\eta \gg 1$ the streaming length L_S is not discernible on the $n_2(\tau)$ distribution, while the decrease of the surface density $n_2(0)$ with increasing ζ is again clearly seen (see Fig. 6). For $\eta \gg 1$ and $\omega_c \gg 1$, the thermalization length L_T is affected by elastic collisions not only indirectly through the destruction of partial redistribution as in the case $\eta \ll 1$, but also directly through the alteration of the particle streaming as predicted by the two-fluid model [cf. Eq. (4.14)].

The various features encountered in the presence of destroying boundaries for $\eta \ll 1$ and $\eta \gg 1$, respectively, are satisfactorily accounted for by the two-fluid model. From Eqs. (4.16), (4.21) (4.22), (II.6.37), and (II.6.38), we derive the surface density

$$n_2^D(0) = \frac{\epsilon^{1/2}}{(1 + \zeta)^{1/2} + (1 + \omega_c^2)^{1/2} - \omega_c + \epsilon^{1/2}\omega_c/(1 + \omega_c^2)^{1/2}}. \tag{4.28}$$

For small $\epsilon \ll 1$ and for $\eta \ll 1$, $\omega_c \ll 1$, this relation reduces to

$$n_2^D(0) \simeq \epsilon^{1/2}/[(1 + \zeta)^{1/2} + 1]; \tag{4.29}$$

similarly, for $\eta \gg 1$, $\omega_c \gg 1$,

$$n_2^D(0) \simeq \epsilon^{1/2}/(1 + \zeta)^{1/2}. \tag{4.30}$$

Comparison with Figs. 5 and 6 shows that Eqs. (4.29) and (4.30) are in reasonable agreement with the numerical solutions.

For $\eta \ll 1$ one has to a first approximation $A_T^D \simeq 1 - \epsilon^{1/2}$ and hence $A_S^D = 1 - A_T^D - n_2^D(0) \simeq \epsilon^{1/2} - n_2^D(0)$, so that from Eq. (4.16)

$$n_2^D(\tau) \simeq 1 - (1 - \epsilon^{1/2})\exp(-\tau/L_T) - [\epsilon^{1/2} - n_2^D(0)]\exp(-\tau/L_S), \tag{4.31}$$

which agrees with Eq. (II.6.57). On the other hand, for $\eta \gg 1$, $A_T^D \simeq 1 - \epsilon^{1/2}(1 + \zeta)^{-1/2}$ or $A_T^D \simeq 1 - n_2^D(0)$ in view of Eq. (4.30), and hence $A_S^D = 1 - A_T^D - n_2^D(0) \simeq 0$, and Eq. (4.16) takes the form

$$n_2^D(\tau) \simeq 1 - [1 - n_2^D(0)]\exp(-\tau/L_T), \tag{4.32}$$

which agrees with Eq. (II.6.59). Equation (4.31) explains the occurrence of the "step" in $n_2(\tau)$ at $\tau \simeq L_S$ in Fig. 5, while Eq. (4.32) accounts for the fact that the scale length L_S is not visible in Fig. 6.

The mean velocity $u(\tau)$ is plotted in Figs. 7 and 8 for the same cases as depicted in Figs. 5 and 6. At the surface one has always $u(0) \simeq 2^{-1/2}$. If $\eta \ll 1$, $u(\tau)$ drops rapidly in the interval $0 < \tau < L_S$, followed by a much slower decrease for $\tau > L_S$ (see Fig. 7). As a result, the streaming length L_S is easily discernible on the $u(\tau)$ distribution, and the decrease of L_S with increasing ζ can again be observed. On the other hand, the slow decay of $u(\tau)$ for $\tau > L_S$ is governed by the thermalization
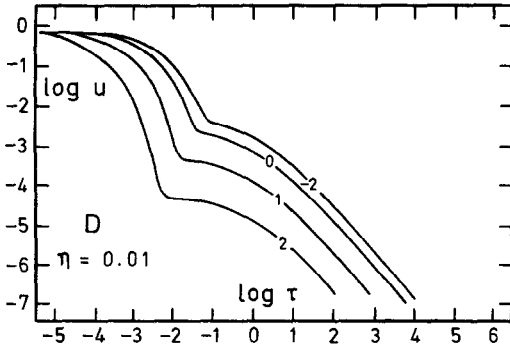
Fig. 7. Mean velocity of excited atoms u vs optical depth τ of a gas layer $\epsilon = 10^{-4}$, $\eta = 0.01$, $\tau^0 = 2 \times 10^6$, with destroying boundaries. Curve labeled n ($n = -2, \ldots, 2$) corresponds to $\zeta = 10^n$.

Fig. 8. Mean velocity of excited atoms u vs optical depth τ of a gas layer $\epsilon = 10^{-4}$, $\eta = 100$, $\tau^0 = 2 \times 10^6$ with destroying boundaries. Curve labeled n ($n = -2, \ldots, 2$) corresponds to $\zeta = 10^n$.
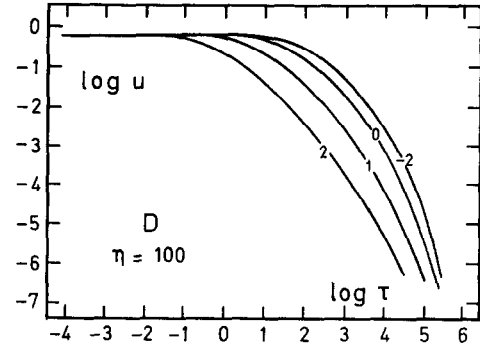
length. That there the $u(\tau)$ curves are nearly parallel corresponds to the fact that L_T is approximately independent of ζ (see also Fig. 5). In the opposite limiting case $\eta \gg 1$, Fig. 8, the streaming length L_S is not visible on the $u(\tau)$ distribution, as it was the case with the $n_2(\tau)$ distribution (see Fig. 6), and the decay of $u(\tau)$ is governed by the thermalization length L_T throughout. Again, it can be seen that L_T decreases with increasing ζ (see Figs. 6 and 8).

The particle flux into a destroying boundary decreases with increasing elastic collision frequency. Indeed, $\phi(0) = n_2(0)\, u(0)$, where $u(0)$ is independent of ζ, while $n_2(0)$ decreases with increasing ζ.

In order to study the influence of elastic collisions on the emission profile ψ_x (and hence on the velocity distribution f_2 too, because f_2 behaves essentially like ψ_x), we consider the reduced emission profile $\tilde{\psi}_x(\mu)$ for the same cases that were discussed in Fig. II. 12 of Part II. For simplicity, we consider the corresponding angle-averaged profiles of outgoing ($\mu > 0$) and incoming ($\mu < 0$) photons defined by

$$\tilde{\psi}_x^+ = \int_0^1 \tilde{\psi}_x(\mu)\, d\mu, \quad \tilde{\psi}_x^- = \int_0^1 \tilde{\psi}(-\mu)\, d\mu, \tag{4.33}$$

which according to Eq. (2.4) are related through

$$\tilde{\psi}_{-x}^+ = \tilde{\psi}_x^- . \tag{4.34}$$

Here we have used the fact that the absorption profile φ_x, Eq. (2.2), which enters $\tilde{\psi}_x$ through $\tilde{\psi}_x(\mu) = \psi_x(\mu)/\varphi_x$, is independent of μ and obeys $\varphi_x = \varphi_{-x}$.

Estimates of the anisotropy of $\psi_x(\mu)$ and hence of $f_2(\mathbf{y})$ may be obtained from Fig. II.12 which corresponds to $\zeta = 0$. For $\zeta \neq 0$, the anisotropy of $\tilde{\psi}_x(\mu)$ at the surface $\tau = 0$ is almost the same as in the collisionless case $\zeta = 0$ because of the identical boundary condition $f_2(y, \mu; \tau = 0) = 0$ for $\mu < 0$. On the other hand, in deeper layers $\tau > 0$, the anisotropy of $\tilde{\psi}_x(\mu)$ is smaller for $\zeta \neq 0$ than for $\zeta = 0$, and decreases with increasing parameter ζ, as expected on physical grounds.

Our results are presented in Fig. 9. Consider first the surface $\tau = 0$ where the mean velocity takes the value $u(0) \simeq 2^{-1/2}$ (see Figs. 7 and 8). As a result, the core of the profiles $\tilde{\psi}_x^+$, which is determined by this macroscopic flow, is practically independent of the parameters η and ζ. On the other hand, the wings of the profiles $\tilde{\psi}_x^+$ show the usual "overpopulation" due to partial redistribution, which is more pronounced for $\eta = 0.01$ than for $\eta = 100$, and which decreases with increasing ζ, as expected.

Let us now follow the depth dependence of $\tilde{\psi}_x^+(\tau)$ in the case $\eta = 0.01$. Figure 7 shows that at the depth $\tau = \eta = 0.01$ the mean velocity is already much smaller than the surface velocity $u(0) \simeq 2^{-1/2}$. As a result, $\tilde{\psi}_x^+$ at $\tau = \eta = 0.01$ is only slightly asymmetric about the line center for $\zeta \ll 1$, and is practically symmetric for $\zeta \gtrsim 1$. At the larger depth $\tau = 1$, the macroscopic velocity is already so small (see Fig. 7) that $\tilde{\psi}_x^+$ is symmetric for all ζ. Consider now the case $\eta = 100$. Here, the macroscopic velocity at $\tau = 1$ is still practically the surface velocity $u(0) \simeq 2^{-1/2}$ as long as $\zeta \lesssim 10$ (see Fig. 8), so that $\tilde{\psi}_x^+$ at $\tau = 1$ differs from $\tilde{\psi}_x^+$ at $\tau = 0$ only for $\zeta > 10$ (see Fig. 9). At the depth
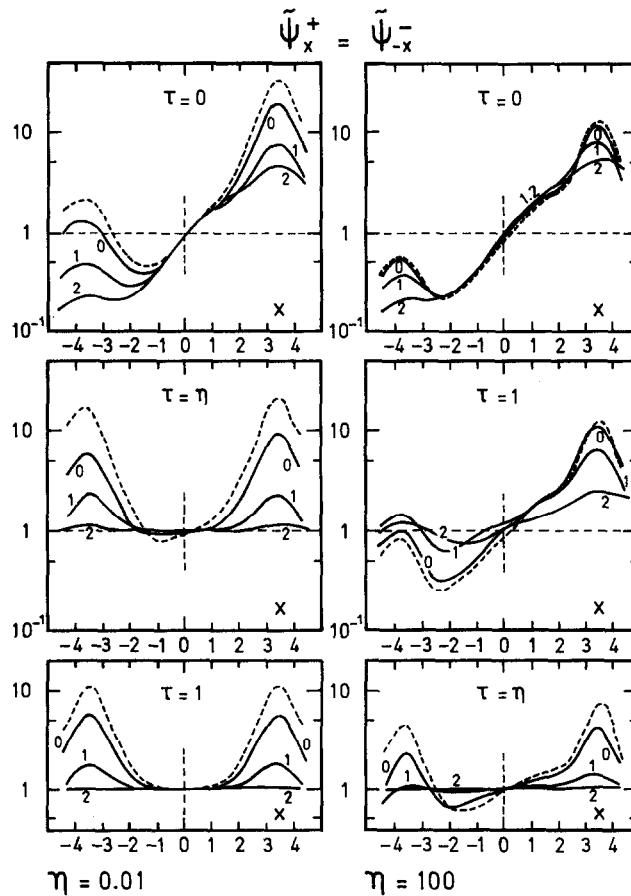
$$\tilde{\psi}_x^+ = \tilde{\psi}_{-x}^-$$

Fig. 9. Angle-average reduced emission profiles $\tilde{\psi}_x^+$ and $\tilde{\psi}_x^-$, Eqs. (4.33) and (4.34), vs frequency x of a gas layer $\epsilon = 10^{-4}$, $\tau^0 = 2 \times 10^6$, with destroying boundaries for $\eta = 0.01$ and 100, at various optical depths τ. Curves labeled n ($n = 0, 1, 2$) correspond to $\zeta = 10^n$, dashed curves to $\zeta = 0$.

$\tau = \eta = 100$, the cases $\zeta = 10$ and 100 in Fig. 9 correspond approximately to complete redistribution, while $\tilde{\psi}_x^+$ for $\zeta \lesssim 1$ still shows the effect of partial redistribution superimposed on a macroscopic flow velocity (cf. Figs. 5–8).

Finally, we turn to the emergent intensity $I_x^+(\mu; \tau = 0)$ for the same cases $\eta = 0.01$ and 100. For $\eta = 0.01$, the streaming of excited atoms is restricted to the very thin surface layer $0 < \tau < L_S \ll 1$, which means that almost all of the layer of line formation $\tau \varphi_x \lesssim 1$ behaves as a static gas (Sec. 3), even in the presence of a destroying boundary. In contrast, for $\eta \gg 1$, streaming of excited atoms is important in the layer of line formation $\tau \varphi_x \lesssim 1$ in a large frequency range about the line center $x = 0$, and thus affects the emergent intensity at these frequencies. Figure 10 shows a plot of the emergent mean intensity at the surface $\tau = 0$, viz.

$$J_x(0) = \frac{1}{2} \int_0^1 I_x(\mu; 0) \, d\mu. \tag{4.35}$$

It can be seen that the core of the emitted spectral line varies as a function of ζ according to the corresponding variation of the surface density $n_2(0)$ (see Fig. 6). Moreover, for $\zeta \lesssim 10$, it is asymmetric about the line center due to particle streaming (see Fig. 8). On the other hand, the line wings, being formed at large optical depths, depend only slightly on ζ, and are symmetric.

5. DIFFUSION APPROXIMATION

In this section we discuss elastic collision-dominated gases in which the excited atoms undergo many elastic velocity-changing collisions during their lifetime, $\zeta \gg 1$. This is the opposite limiting
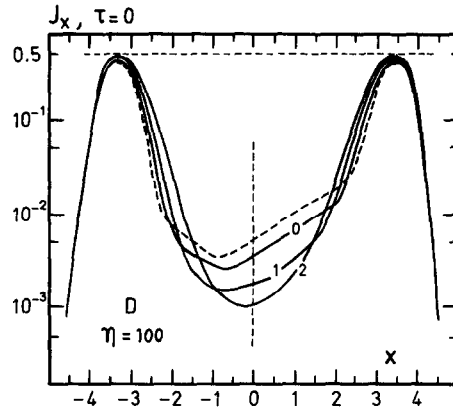
Fig. 10. Emerging mean intensity $J_x(\tau = 0)$, Eq. (4.35), vs frequency x of a gas layer $\epsilon = 10^{-4}$, $\eta = 100$, $\tau^0 = 2 \times 10^6$, with destroying boundaries. Curve labeled n ($n = 0, 1, 2$) corresponds to $\zeta = 10^n$, dashed curve to $\zeta = 0$. For comparison: a blackbody radiator $I_x^+(\mu) = 1$ emits $J_x = 0.5$.

case to the situation considered in Part II where such elastic collisions were negligible, $\zeta \ll 1$. Intuitively, it is clear that for $\zeta \gg 1$ complete redistribution is approached, and that streaming of excited atoms is described by a diffusion flow (as opposed to free particle streaming in the case $\zeta \ll 1$), except in a thin surface layer near a destroying boundary where the macroscopic flow velocity is always of the order of the thermal velocity of the atoms (see Sec. 4.3). In the following we develop an approximate method of solving the coupled kinetic equations for the excited atoms and the photons, referred to as the diffusion approximation, which applies if simultaneously the two inequalities

$$\zeta \gg 1, \quad \eta/\zeta \ll 1 \tag{5.1}$$

hold. In view of Eqs. (II.2.2) and (II.2.3), the first inequality expresses the fact that the mean path length traveled by an excited atom in much smaller than the gas-kinetic mean free path ($\lambda_{exc} \ll \lambda_{el}$), and the second, that the mean free path of the excited atoms is much smaller than the mean path length traveled by the photon ($\lambda_{el} \ll \lambda_{ph}$). Since the scale length of gradients due to non-LTE line transfer is of the order of λ_{ph}, the second inequality is therefore a necessary condition for a diffusion regime to apply, which requires that the mean free path is small compared to the scale length of the gradients.

The starting point is the kinetic equation (2.5a) which upon integration over all velocities y yields [cf. Eqs. (II.3.37) and (2.8)]

$$\eta \, d\phi/d\tau = n_2 - [\epsilon + (1 - \epsilon)J_{12}]. \tag{5.2}$$

In the diffusion approximation, the flux density is proportional to the density gradient, $\phi \propto dn_2/d\tau$ [see Eq. (5.15)], thus leading to a second order diffusion equation for n_2 [see Eq. (5.17)] (cf. also Sec. I.4).

5.1. The diffusion approximation

We start from the kinetic equation (2.5b) of the excited atoms, which we write as

$$F_2(y) = \frac{1}{1 + \zeta} [\epsilon + (1 - \epsilon)I_{12}(y) + \zeta n_2] f^M(y) + \frac{\eta y \mu'}{1 + \zeta} \frac{d}{d\tau} F_2(y). \tag{5.3}$$

Here and in the following, we distinguish explicitly between the direction cosines referring to the atoms and the photons, respectively. That is, as in Secs. 4.1, II.3.2, and II.6.1, we designate $\mu' \equiv \mathbf{y} \cdot \mathbf{e}_z/y$ and $\mu \equiv \mathbf{n} \cdot \mathbf{e}_z$.

We now introduce two approximations in Eq. (5.3). First, in accord with Eq. (5.1), we put $(1 + \zeta)^{-1} \simeq \zeta^{-1}$, $\zeta/(1 + \zeta) \simeq 1 - \zeta^{-1}$, $\eta/(1 + \zeta) \simeq \eta/\zeta$. And second, in the last term of Eq. (5.3) which is small because it contains the factor $\eta/\zeta \ll 1$, we set $F_2(y) \simeq n_2 f^M(y)$ which is expected to hold in an elastic collision-dominated gas except in a thin surface layer near a destroying boundary.

We thus obtain the (approximate) distribution function

$$F_2(\mathbf{y}) = n_2 f^M(y) + \frac{1}{\zeta} [\epsilon + (1-\epsilon) I_{12}(\mathbf{y}) - n_2] f^M(y) + \frac{\eta}{\zeta} \frac{dn_2}{d\tau} y\mu' f^M(y). \qquad (5.4a)$$

Performing here the integration $\int d^3 y$ and taking Eq. (2.8) into account leads to the (approximate) density

$$n_2 = \epsilon + (1-\epsilon) J_{12}$$

[cf. Eq. (3.2)], which, when substituted back into Eq. (5.4a), yields the distribution function

$$F_2(\mathbf{y}) = n_2 f^M(y) + \frac{1-\epsilon}{\zeta} [I_{12}(\mathbf{y}) - J_{12}] f^M(y) + \frac{\eta}{\zeta} \frac{dn_2}{d\tau} y\mu' f^M(y). \qquad (5.4b)$$

Here, in analogy to Eq. (3.3), the first term on the r.h.s. corresponds to static complete redistribution, while the second and third terms are correction terms due to partial redistribution and streaming of the excited atoms, respectively.

On the other hand, the line emission coefficient $n_2 \psi_x(\mathbf{n})$ corresponding to the distribution function (5.4b) follows from Eq. (2.3). Taking Eqs. (II.4.6), (3.9), (3.10), and (II.3.44) into account, one obtains

$$n_2 \psi_x(\mathbf{n}) = n_2 \varphi_x + \frac{1-\epsilon}{\zeta} [R_x(\mathbf{n}) - J_{12}\varphi_x] + \frac{\eta}{\zeta} \frac{dn_2}{d\tau} x\mu\varphi_x. \qquad (5.5)$$

Again, by analogy to Eq. (3.8), the first term on the r.h.s. corresponds to complete redistribution, while the second and third terms are correction terms due to partial redistribution and streaming of the excited atoms, respectively.

In Eqs. (5.4b) and (5.5) the corrections terms due to partial redistribution and streaming are small since they contain the small factors $1/\zeta$ and η/ζ, Moreover, their mean values vanish,

$$\int [I_{12}(\mathbf{y}) - J_{12}] f^M(y) \, d^3 y = 0, \qquad \int y\mu' f^M(y) \, d^3 y = 0, \qquad (5.6)$$

$$\iint [R_x(\mathbf{n}) - J_{12}\varphi_x] \, dx \, d\Omega/4\pi = 0, \qquad \iint x\mu\varphi_x \, dx \, d\Omega/4\pi = 0, \qquad (5.7)$$

using Eqs. (2.8), (3.11), and (3.12).

We now introduce a last approximation by requiring that the distribution function $F_2(\mathbf{y})$, Eq. (5.4b), be determined using a radiation field that corresponds to a static gas. In a static gas (that is, in the absence of particle streaming), the radiation intensity is symmetric about the line center [cf. Eq. (II.4.7)]

$$I_x^0(\mu) = I_{-x}^0(\mu), \qquad (5.8)$$

and the emission profile obeys the symmetry relations [cf. Eqs. (II.4.8) and (2.4)]

$$\psi_x^0(\mu) = \psi_{-x}^0(\mu), \qquad (5.9a)$$

$$\psi_x^0(\mu) = \psi_x^0(-\mu), \qquad (5.9b)$$

where the superscript 0 refers to the static case.

The justification of this approximation derives from the following consideration. The nonstatic (asymmetric) part of the radiation intensity is due to the nonstatic part of the partial redistribution term of $\psi_x(\mathbf{n})$, on the one hand, and the streaming term of $\psi_x(\mathbf{n})$, on the other, which are of the order of $1/\zeta$ and η/ζ, respectively. Inserted into Eq. (5.4b), they give rise to contributions proportional to ζ^{-2} which are neglected in the diffusion approximation.

Thus, the line emission coefficient in the diffusion approximation reads [cf. Eq. (5.5)]

$$n_2 \psi_x^0(\mathbf{n}) = n_2 \varphi_x + [(1-\epsilon)/\zeta][R_x^0(\mathbf{n}) - J_{12}^0 \varphi_x], \qquad (5.10)$$

which obeys Eqs. (5.9a,b). Here, $R_x^0(\mathbf{n})$ and J_{12}^0 are defined by Eq. (3.9) and (2.8), there using the static intensity $I_x^0(\mathbf{n})$ which obeys Eq. (5.8). We remark that using the static emission coefficient

(5.10) in the transfer equation (2.1) automatically yields the static intensity $I_x^0(\mathbf{n})$ since the absorption coefficient (2.2) corresponds to the static Maxwell distribution $F_1(\mathbf{v}) = n_1 f^M(v)$, Eq. (I.2.4).

On the other hand, the distribution function of excited atoms is now given by [cf. Eq. (5.4b)]

$$F_2(\mathbf{y}) = F_2^0(\mathbf{y}) + (\eta/\zeta)(dn_2/d\tau) y \mu' f^M(y). \tag{5.11}$$

Here

$$F_2^0(\mathbf{y}) = n_2 f^M(y) + [(1-\epsilon)/\zeta][I_{12}^0(\mathbf{y}) - J_{12}^0] f^M(y), \tag{5.12}$$

which obeys the symmetry relation [cf. Eq. (II.4.10)]

$$F_2^0(y, \mu) = F_2^0(y, -\mu). \tag{5.13}$$

In Eq. (5.12), $I_{12}^0(\mathbf{y})$ and J_{12}^0 are defined by Eqs. (2.7) and (2.8), there using the static intensity $I_x^0(\mathbf{n})$. We note that

$$\int F_2(\mathbf{y}) \, d^3 y = \int F_2^0(\mathbf{y}) \, d^3 y = n_2. \tag{5.14}$$

The distribution function (5.11) leads according to Eq. (II.3.37) to the flux density of excited atoms

$$\phi = (\eta/2\zeta) \, dn_2/d\tau \tag{5.15}$$

because the static part F_2^0 does not contribute on account of Eq. (5.13). Here the minus sign of the usual expression $\phi = -D\nabla n$ is missing due to the definition of τ, Eq. (I.2.48). On the other hand, Eq. (5.2) now takes the form

$$\eta \, d\phi/d\tau = n_2 - [\epsilon + (1-\epsilon) J_{12}^0]. \tag{5.16}$$

Combining Eqs. (5.15) and (5.16) leads to the diffusion equation for the density of excited atoms n_2 [see Eq. (I.4.14) where $\tilde{I}_{12}$ should read $\tilde{J}_{12}$]

$$n_2(\tau) - \delta n_2''(\tau) = \epsilon + (1-\epsilon) J_{12}^0(\tau) \tag{5.17}$$

if here and in the following a prime ′ stands for $d/d\tau$, and [see Eq. (I.4.15)]

$$\delta = \eta^2/2\zeta. \tag{5.18}$$

To derive the boundary conditions at $\tau = 0$, consider the density of outgoing ($\mu' > 0$) excited atoms

$$n_2^+ = 2\pi \int_0^\infty y^2 \, dy \int_0^1 F_2(y, \mu') \, d\mu'. \tag{5.19}$$

According to Eq. (5.11) it obeys the relation

$$n_2^+ = \tfrac{1}{2} n_2 + (2\pi^{1/2})^{-1} (\eta/\zeta) \, dn_2/d\tau, \tag{5.20}$$

where Eqs. (5.13) and (5.14) have been used to obtain the first term on the r.h.s. Now, at a reflecting boundary at $\tau = 0$, $n_2^+(0) = \tfrac{1}{2} n_2(0)$, while at a destroying boundary at $\tau = 0$, $n_2^+(0) = n_2(0)$. Therefore, using Eq. (5.20), the boundary condition at $\tau = 0$ takes the form

$$n_2'(0) = \gamma n_2(0); \quad \gamma^R = 0, \quad \gamma^D = \pi^{1/2} \zeta/\eta. \tag{5.21}$$

In terms of the mean velocity $u = \phi/n_2 = (\eta/2\zeta) n_2'/n_2$ [cf. Eq. (5.13)], this means

$$u^R(0) = 0, \quad u^D(0) = \tfrac{1}{2}\pi^{1/2}. \tag{5.22}$$

Above, the superscripts R and D stand again for reflecting and destroying boundaries, respectively.

Turning now to the radiation field, the transfer equation for the static intensity $I_x^0(\mathbf{n})$ is [see Eq. (2.1)]

$$\mu(d/d\tau) I_x^0(\mu) = \varphi_x I_x^0(\mu) - n_2 \psi_x^0(\mu) \tag{5.23}$$

with $n_2\psi_x^0$ given by Eq. (5.10). In terms of outgoing ($\mu > 0$). and incoming ($\mu < 0$) intensities [see Eq. (I.2.52)]

$$\mu(\mathrm{d}/\mathrm{d}\tau)I_x^+(\mu) = \varphi_x I_x^+(\mu) - n_2\psi_x^0(\mu), \tag{5.24a}$$

$$-\mu(\mathrm{d}/\mathrm{d}\tau)I_x^-(\mu) = \varphi_x I_x^-(\mu) - n_2\psi_x^0(\mu), \tag{5.24b}$$

where $\mu > 0$, and where Eq. (5.9b) has been used in Eq. (5.24b). Defining now [no confusion with Eqs. (II.3.20–21) should arise]

$$J_x(\mu) = \tfrac{1}{2}[I_x^+(\mu) + I_x^-(\mu)], \quad H_x(\mu) = \tfrac{1}{2}[I_x^+(\mu) - I_x^-(\mu)], \tag{5.25}$$

one obtains from Eqs. (5.24)

$$\mu(\mathrm{d}/\mathrm{d}\tau)H_x(\mu) = \varphi_x J_x(\mu) - n_2\psi_x^0(\mu), \tag{5.26a}$$

$$\mu(\mathrm{d}/\mathrm{d}\tau)J_x(\mu) = \varphi_x H_x(\mu), \tag{5.26b}$$

leading to the second order differential equation for $J_x(\mu)$

$$\mu^2 J_x''(\mu; \tau) = \varphi_x^2 J_x(\mu; \tau) - \varphi_x n_2(\tau)\psi_x^0(\mu; \tau). \tag{5.27}$$

The boundary condition at $\tau = 0$ is $I_x^-(\mu) = 0$ and hence $J_x(\mu) = H_x(\mu)$, which in view of Eq. (5.26b) can be written as

$$\mu J_x'(\mu; 0) = \varphi_x J_x(\mu; 0). \tag{5.28}$$

We recall that

$$J_x(\mu; \tau) = J_{-x}(\mu; \tau) \tag{5.29}$$

because of Eq. (5.8), so that [see Eqs. (2.8) and (3.9)]

$$J_{12}^0(\tau) = 2\int_0^\infty \mathrm{d}x \int_0^1 \mathrm{d}\mu\, \varphi_x J_x(\mu; \tau), \tag{5.30}$$

$$R_x^0(\mu; \tau) = 2\int_0^\infty \mathrm{d}x' \int_0^1 \mathrm{d}\mu'\, J_{x'}(\mu'; \tau)R_{\mathrm{IA}}(x', \mu'; x, \mu), \tag{5.31}$$

with the redistribution function R_{IA} given by Eq. (3.10).

To sum up, the diffusion approximation consists of the diffusion equation (5.17) with boundary condition (5.21) for the density n_2, and the transfer equation (5.27) with boundary condition (5.28) for the intensity J_x. These two equations are coupled to each other through Eqs. (5.10), (5.30), and (5.31).

5.2. Method of solution and results

We have solved the coupled diffusion and transfer equations, Eqs. (5.17) and (5.27), for a gas layer specified by

$$\epsilon = 10^{-4}, \quad \tau^0 = \infty,$$

rather than $\tau^0 = 2 \times 10^6$ as considered previously. The differences between these two cases are negligible, apart from the fact that the emergent spectral line of the semi-infinite medium has the shape of an absorption line, whereas that of the layer of finite optical thickness has the shape of a (double-humped) emission line.

In order to solve Eqs. (5.17) and (5.27) we have employed the method of discrete ordinates. Choosing F positive frequencies x_i ($i = 1, \ldots, F$) and D positive direction cosines μ_j ($j = 1, \ldots, D$), and writing for brevity $J_{ij} \equiv J_{x_i}(\mu_j)$, $\psi_{ij} \equiv \psi_{x_i}^0(\mu_j)$, $\varphi_i \equiv \varphi_{x_i}$, we write Eq. (5.30) in discrete form as

$$J_{12}^0(\tau) = \sum_{i,j} W^i J_{ij}(\tau), \tag{5.32}$$

and Eq. (5.10) on account of Eq. (5.31) as

$$n_2(\tau)\psi_{ij}(\tau) = n_2(\tau)\varphi_i + [(1 - \epsilon)/\zeta]\varphi_i \sum_{i',j'} (R_{ij}^{i'j'} - W^{i'})J_{i'j'}(\tau). \tag{5.33}$$

Here the integration weights W^i and $R_{ij}^{i'j'}$ correspond to the quantities φ_x and R_{1A}/φ_x, respectively, and they are normalized according to

$$\sum_{i,j} W^i = \sum_{i',j'} R_{ij}^{i'j'} = 1 \qquad (5.34)$$

in view of the normalizations (I.2.28) and (3.12). We notice that the normalization of W^i includes a summation over $j = 1, \ldots, D$ (that is, it contains the factor D).

For a semi-infinite gas layer, we therefore have the following system of equations [see Eqs. (5.17), (5.21), (5.27), (5.28)]

$$n_2(\tau) - \delta n_2''(\tau) = \epsilon + (1 - \epsilon) \sum_{i,j} W^i J_{ij}(\tau), \qquad (5.35)$$

$$\mu_j^2 J_{ij}''(\tau) = \varphi_i^2 \left[J_{ij}(\tau) - n_2(\tau) - \frac{1 - \epsilon}{\zeta} \sum_{i',j'} (R_{ij}^{i'j'} - W^{i'}) J_{i'j'}(\tau) \right], \qquad (5.36)$$

$$n_2(\infty) = J_{ij}(\infty) = 1, \qquad (5.37)$$

$$n_2'(0) = \gamma n_2(0); \quad \gamma^R = 0, \quad \gamma^D = \pi^{1/2} \zeta / \eta, \qquad (5.38)$$

$$\mu_j J_{ij}'(0) = \varphi_i J_{ij}(0). \qquad (5.39)$$

These are $FD + 1$ equations with appropriate boundary conditions for the $FD + 1$ unknowns (1 density n_2, FD intensities J_{ij}). The flux density ϕ and the mean velocity u follow from the density n_2 according to [see Eq. (5.15)]

$$\phi(\tau) = (\eta / 2\zeta) n_2'(\tau), \quad u(\tau) = \phi(\tau) / n_2(\tau). \qquad (5.40)$$

To solve Eqs. (5.35)–(5.39), we write

$$n_2(\tau) = 1 - \sum_k N_k \exp(-\lambda_k \tau) \qquad (5.41)$$

$$J_{ij}(\tau) = 1 - \sum_k N_k g_{ijk} \exp(-\lambda_k \tau). \qquad (5.42)$$

Here the sum over k runs from $k = 1$ to $FD + 1$. The $FD + 1$ numbers λ_k must be positive on account of the boundary condition (5.37).

Inserting now Eqs. (5.41) and (5.42) into the transfer equation (5.36) and taking Eq. (5.34) into account yields

$$g_{ijk}(\mu_j^2 \lambda_k^2 - \varphi_i^2) + \varphi_i^2 + [(1 - \epsilon)/\zeta] \sum_{i',j'} (R_{ij}^{i'j'} - W^{i'}) g_{i'j'k} = 0. \qquad (5.43)$$

In the diffusion approximation which neglects terms proportional to ζ^{-2}, we may replace in the last term of the r.h.s. the quantity $g_{i'j'k}$ by its value corresponding to complete redistribution ($\zeta = \infty$). We then obtain

$$g_{ijk} = \frac{\varphi_i^2}{\varphi_i^2 - \mu_j^2 \lambda_k^2} + \frac{1 - \epsilon}{\zeta} \frac{1}{\varphi_i^2 - \mu_j^2 \lambda_k^2} \sum_{i',j'} (R_{ij}^{i'j'} - W^{i'}) \frac{\varphi_{i'}^2}{\varphi_{i'}^2 - \mu_j^2 \lambda_k^2}, \qquad (5.44)$$

which is correct up to the order ζ^{-1}.

On the other hand, inserting Eqs. (5.41) and (5.42) into the diffusion equation (5.35) and taking Eq. (5.34) into account yields

$$1 - \delta \lambda_k^2 - (1 - \epsilon) \sum_{i,j} W^i g_{ijk} = 0. \qquad (5.45)$$

Substituting Eq. (5.44) into Eq. (5.45) now leads to the characteristic equation

$$1 - \delta \lambda_k^2 - (1 - \epsilon) \sum_{i,j} W^i \frac{\varphi_i^2}{\varphi_i^2 - \mu_j^2 \lambda_k^2}$$
$$- \frac{(1 - \epsilon)^2}{\zeta} \sum_{i,j} W^i \frac{\varphi_i^2}{\varphi_i^2 - \mu_j^2 \lambda_k^2} \sum_{i',j'} (R_{ij}^{i'j'} - W^{i'}) \frac{\varphi_{i'}^2}{\varphi_{i'}^2 - \mu_j^2 \lambda_k^2} = 0, \qquad (5.46)$$
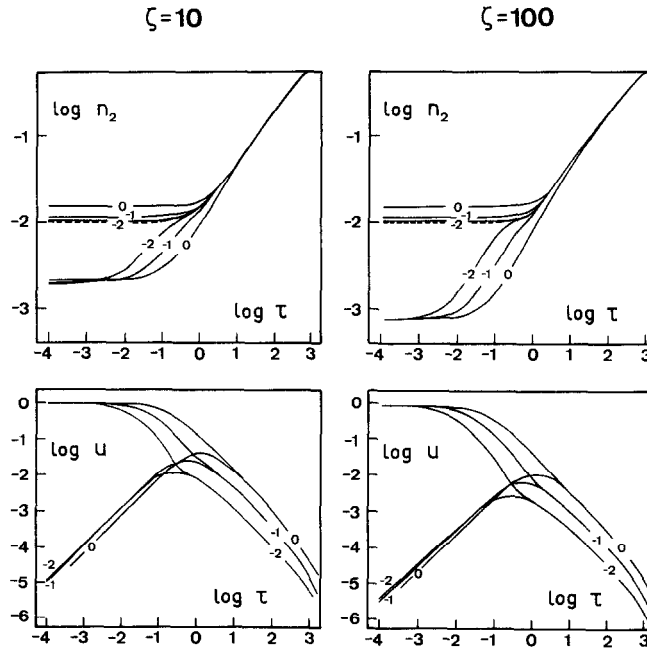
$\zeta = 10$ $\zeta = 100$

Fig. 11. Density of excited atoms n_2 and mean velocity u of excited atoms vs optical depth τ of a semi-infinite gas layer with $\epsilon = 10^{-4}$, with reflecting and destroying boundaries, respectively. Curves labeled n ($n = -2, -1, 0$) correspond to $\delta = 10^n$, Eq. (5.18). The calculations have been performed using the diffusion approximation, Sec. 5. The dashed curve for n_2 corresponds to static complete redistribution ($\delta = 0$, $\zeta = \infty$). In the case $\zeta = 10$, $\delta = 1$, the condition $\eta/\zeta \ll 1$, Eq. (5.1), is not well satisfied.

from which the positive λ_k's ($k = 1, \ldots, FD + 1$) are to be determined. In Eq. (5.46), the second and fourth terms are due to particle streaming and partial redistribution, respectively. Setting $\delta = 0$ and $\zeta = \infty$, one recovers, of course, the characteristic equation for static complete redistribution.

Having calculated the $FD + 1$ positive λ_k's as solutions of Eq. (5.46) one determines the $FD + 1$ constants N_k in Eqs. (5.41) and (5.42) from the boundary conditions (5.38) and (5.39), that is, as solutions of the $FD + 1$ equations

$$\sum_k N_k \lambda_k = \gamma \left(1 - \sum_k N_k \right),$$ (5.47)

$$\mu_j \sum_k N_k g_{ijk} \lambda_k = \varphi_i \left(1 - \sum_k N_k g_{ijk} \right),$$ (5.48)

where g_{ijk} is given by Eq. (5.44). This completes the solution of Eqs. (5.35–39).

Some numerical results are shown in Fig. 11 for the cases $\zeta = 10$ and 100. The behavior of an elastic collision-dominated gas of excited atoms in the surface layer $0 < \tau < L_S$ is again determined by the boundary condition. The various features seen in Fig. 11 are to a large extent explained by the two-fluid model of Sec. 4, carrying out the substitutions

$$1 + \zeta \to \zeta, \quad \omega_c \to \delta^{1/2}/\beta \sim \delta^{1/2}$$

in agreement with the diffusion approximation.

It should be observed that for $\zeta \gg 1$, only a gas confined by a reflecting boundary is in a true diffusion regime where the macroscopic gas velocity is small compared with the thermal speed of the atoms, and where the particle flow is described by a diffusion flow due to density gradients.[6,7] In a diffusion regime, the density of excited atoms is specified by only two parameters ϵ and δ (see Sec. I.4), ignoring a very slight dependence on the parameter ζ due to partial redistribution which vanishes for $\zeta \to \infty$. By contrast, in the neighborhood of a destroying boundary, the density of excited atoms depends even in a collision-dominated regime on all three parameters ϵ, δ, ζ (or, equivalently, on ϵ, η, ζ), as can be seen in Fig. 11. This different behaviour can formally be traced back to the boundary condition (5.21) where for a destroying boundary the ratio ζ/η arises, in

contrast to a reflecting boundary. Hence, apart from the parameter ϵ, two different quantities η^2/ζ [in Eq. (5.35)] and η/ζ [in Eq. (5.38)] intervene in the case of a destroying boundary.

For numerical results for the case of important diffusion flow ($\delta \gg 1$ with reflecting boundaries) we refer to Ref. 7.

6. DISCUSSION

Our study has reconsidered the classic problem of non-LTE line transfer by two-level atoms in a stationary and homogeneous gas. Our approach supposes the distribution functions of nonexcited atoms and free electrons to be known, so that only the distribution function of excited atoms and the specific intensity of the radiation field are to be determined from the kinetic equation of the excited atoms and the radiative transfer equation, respectively. These two equations are coupled to each other through the various source and sink terms of excited atoms and photons. In constrast to the usual approach, we take into account the streaming of the excited atoms, on the one hand, and the occurrence of elastic collisions of the excited atoms, on the other. These two phenomena give rise to two new dimensionless parameters η and ζ that characterize the streaming and the elastic collisions, respectively. Together with the well-known dimensionless parameter ϵ that characterizes the inelastic collisions, they specify the gas of two-level atoms under consideration.

Taking particle streaming into account leads to a differential equations for the distribution function of excited atoms which must be supplemented by boundary conditions. We have discussed the two limiting cases of reflecting and destroying boundaries for the excited atoms. In this context, a new scale length arises, the so-called streaming length L_S, which constitutes a second characteristic scale length of the radiative tranfer problem considered, in addition to the well-known thermalization length of the photons L_T.

In our paper we have considered only the case of pure Doppler broadening. We now present arguments that make it plausible that the streaming pattern of the gas of excited atoms is rather insensitive to the shape of the line profile, so that our results for pure Doppler broadening may also be used for other line profiles (Voigt, Lorentz) in a first approximation.

It is well known that the thermalization length is determined by the radiation transfer in the line wings, and therefore depends very critically on the shape of the line profile. By contrast, the radiation field near the boundary is determined by the radiative transfer in the line core and is practically independent of the line profile, leading to a radiation intensity whose depth variation is governed by a scale length of the order of $\epsilon^{-1/2}$. In view of the fact that particle streaming arises primarily in these boundary layers, this suggests that the streaming properties of the gas of excited atoms should be largely independent of the line profile because the value of the normalized profile coefficient near the line center is always of the order of unity.

More precisely, the streaming length L_S^0 in a given radiation field (that is, disregarding the influence of particle streaming on the radiation transport) is according to Eq. (4.3) of the order of α_c, or, on account of Eq. (4.11),

$$L_S^0 \sim \eta(1 + \zeta)^{-1/2}. \tag{6.1}$$

On the other hand, as already mentioned, the scale length of the radiation field near the boundary is of the order of $\epsilon^{-1/2}$. Therefore, if $\eta(1 + \zeta)^{-1/2} < \epsilon^{-1/2}$ the streaming interval $0 < \tau < L_S^0$ lies inside the boundary layer $0 < \tau < \epsilon^{-1/2}$ where the radiation field is practically independent of the particular line profile considered. It is thus reasonable to assume that all of our results for Doppler broadening (except the thermalization behavior at large optical depths) will also apply to Voigt and Lorentz profiles in a first approximation as long as $\eta(1 + \zeta)^{-1/2} < \epsilon^{-1/2}$. For larger values of η such that $\eta(1 + \zeta)^{-1/2} > \epsilon^{-1/2}$, the streaming interval $0 < \tau < L_S^0$ comprises optical depths $\tau > \epsilon^{-1/2}$ where radiative transfer in the line wings plays a role, so that in this case, differences between Doppler, Voigt, and Lorentz broadened lines are to be expected.

This argument is also corroborated by the two-fluid model. Indeed, leaving aside the question of the absolute magnitudes of the scale lengths L_T and L_S, the success of the two-fluid model with the choice $\beta \sim 1$ (see Eq. (4.11)] shows that the hydrodynamic properties of the gas of excited atoms (surface density, maximum flow velocity, one- or two-exponential behavior, etc.) are mainly determined by the line transfer in the line core.

In order to get some estimate of the actual values of the thermalization and streaming lengths for a general line profile, we employ the two-fluid model by choosing the representative photon frequency such that the thermalization length in the absence of particle streaming L_T^0 is reproduced [see also Sec. II.6.1], namely,[8]

$$L_T^0 \sim \begin{cases} \epsilon^{-1} & \text{Doppler,} \\ a\epsilon^{-2}(\epsilon < a < 1) & \text{Voigt,} \\ \epsilon^{-2} & \text{Lorentz.} \end{cases} \quad (6.2)$$

Thus, on account of Eq. (II.6.19) and recalling that $\beta = \bar{\mu}/\varphi_{\bar{x}}$ [Eq. (4.2)],

$$\beta \sim \epsilon^{1/2} L_T^0.$$

From Eq. (4.10) and recalling that $L_S^0 \sim \alpha_c$, one gets

$$\omega_c = \alpha_c/\beta \sim L_S^0/\epsilon^{1/2} L_T^0,$$

and Eqs. (4.12) and (4.13) now yield the scale lengths

$$L_T \sim L_T^0 \left[1 + \frac{1}{\epsilon} \left(\frac{L_S^0}{L_T^0} \right)^2 \right]^{1/2}, \quad (6.3a)$$

$$L_S \sim L_S^0 \left[1 + \frac{1}{\epsilon} \left(\frac{L_S^0}{L_T^0} \right)^2 \right]^{-1/2}, \quad (6.3b)$$

where L_S^0 and L_T^0 are given by Eqs. (6.1) and (6.2), respectively. In particular, if $\eta(1 + \zeta)^{-1/2} < \epsilon^{-1/2}$,

$$L_T \sim L_T^0, \quad L_S \sim L_S^0, \quad L_S/L_T \ll 1$$

for all three profiles. For Doppler broadening, the estimates (6.3) are in fair agreement with the numerical results. It would be desirable, of course, to test these estimates by numerical calculations for the other profiles as well.

In an elastic collision-dominated gas, the influence of the boundary on the behavior of the gas of excited atoms pertains in the neighborhood of the boundary. In deeper layers, however, a diffusion regime is attained which is characterized by the dimensionless parameter $\delta = \eta^2/2\zeta$. In the limit $\zeta \to \infty$, complete redistribution is approached everywhere, except in a surface layer near a destroying boundary whose thickness, however, tends to zero.

The physical significance of the three dimensionless parameters ϵ, ζ, η for the considered problem of non-LTE line transfer by two-level atoms can be summarized as follows:

$\epsilon = 1$ LTE
$\epsilon \ll 1$ non-LTE

      $\zeta \ll 1$ kinetic regime (elastic collisions negligible)
           $\eta \ll 1$ static partial redistribution
           $\eta \gg 1$ kinetic flow (free particle streaming)
      $\zeta \gg 1$ diffusion regime (elastic collisions important)
           $\eta \ll 1$ static complete redistribution
           $\eta \gg 1$ $\delta = \eta^2/2\zeta$
                $\delta \ll 1$ static complete redistribution
                $\delta \gg 1$ diffusion flow.

REFERENCES

1. J. Borsenberger, J. Oxenius and E. Simonneau, *JQSRT* **35**, 303 (1986).
2. J. Borsenberger, J. Oxenius and E. Simonneau, *JQSRT* **37**, 331 (1987).
3. J. Oxenius, *JQSRT* **5**, 771 (1965).
4. J. Oxenius, *Kinetic Theory of Particles and Photons*. Springer, Berlin (1986).
5. D. G. Hummer, *Mon. Not. R. astr. Soc.* **125**, 21 (1962).
6. D. F. Düchs and J. Oxenius, *Z. Naturf.* **32a**, 156 (1977).
7. D. F. Düchs, S. Rehker and J. Oxenius, *Z. Naturf.* **33a**, 124 (1978).
8. E. H. Avrett and D. G. Hummer, *Mon. Not. R. astr. Soc.* **130**, 295 (1965).